The method of fundamental solutions for computing acoustic interior transmission eigenvalues

Andreas Kleefeld & Lukas Pieronek‡

Forschungszentrum Jülich GmbH, Jülich Supercomputing Centre, 52425 Jülich, Germany

E-mail: a.kleefeld@fz-juelich.de and l.pieronek@fz-juelich.de

Accepted at Inverse Problems; Preprint

Abstract. We analyze the method of fundamental solutions (MFS) in two different versions with focus on the computation of approximate acoustic interior transmission eigenvalues in 2D for homogeneous media. Our approach is mesh- and integration free, but suffers in general from the ill-conditioning effects of the discretized eigenoperator which we could then successfully balance using an approved stabilization scheme. Our numerical examples cover many of the common scattering objects and prove to be very competitive in accuracy with the standard methods for PDE-related eigenvalue problems. We finally give an approximation analysis for our framework and provide error estimates which bound interior transmission eigenvalue deviations in terms of some generalized MFS output.

Keywords: interior transmission eigenvalues, method of fundamental solutions, non-linear eigenvalue problem

1. Introduction

Interior transmission eigenvalues (ITEs) arise in the study of inverse scattering problems and were first introduced by Colton & Monk [19] and Kirsch [32]. They are related to non-scattering response of specific incident waves which undergo a localized transition of media with varying material properties. Therefore, ITEs can be seen as fingerprints of an opaque object which recover information about its interior. As such their investigation can be applied in many fields of current research such as in non-destructive testing to detect inner integrities and abnormalities of heterogeneous materials, see [9], or in medical imaging for organic tissue analysis, see [13]. We refer to [10] for further discussions and applications. Altogether the accurate and fast calculation of ITEs for arbitrary scattering shapes is a desired task in current disciplines.

The underlying eigenoperator is associated to a system of Helmholtz-type equations defined on the geometric support of the bounded scatterer and imposes

‡ Corresponding author

coupled boundary data which makes the problem non-selfadjoint and non-elliptic. Therefore, the characterization of ITEs requires an individual mathematical treatment since standard approaches like those of elliptic theory are not applicable. New methods such as the (generalized) linear sampling method, see [12, 2, 11], the factorization method, see [33], and the inside outside duality method, see [34, 37], were developed which gave deeper insights into the inverse scattering problem. From a numerical point of view, techniques gained from these findings, but also the usual PDE solving tools like finite element methods, see [43, 20, 7, 31, 30, 44, 40, 39, 28, 51, 54, 53, 26, 24, 29, 27, 52, 49, 38, 47, 48], or boundary integral equations, see [21, 22, 36, 55, 35], are applicable and commonly used for ITEs. However, they either require the solution of regularized inverse problems, or they include the generation of a computational grid for the mathematical discretization of the scatterer followed by numerical integrations of singular kernels or of many test functions, respectively, which make these strategies in special cases too generic and numerically expensive.

In this paper, we want to present two further but simple, mesh- and integration-free alternatives both of which use the Method of Fundamental Solution (MFS) with prescribed source point locations as basic concept in order to compute acoustic ITEs for isotropic, penetrable and homogeneous media in 2D. As a Trefftz-like collocation method, the (discrete) MFS focuses on superposing a family of global solutions to the targeted PDE from a given boundary value problem in order to fulfill the assigned boundary data at selected boundary collocation points. For our purposes this interpolation procedure then translates into a non-linear eigenproblem whose matrix coefficients are holomorphic in the wave number. Our first method will make use of this property for enabling Beyn's algorithm from [6] as ultimate solution device to finally recover approximate interior transmission eigenvalues including multiplicities within a given contour in the complex plane. The latter was applied with respect to transmission problems for the first time in [35] under boundary element methods and proved great success for simple scattering objects in 3D. The main drawback is that our MFS-based eigenproblem then becomes drastically ill-conditioned when the number of trial functions exceeds a certain moderate threshold.

In order to circumvent this lack of conditioning, in a second attempt we try to reuse an approach similar to the extended method of particular solutions (MPS) suggested by Betcke & Trefethen in [5] in the context of Laplacian eigenvalues. Their idea to free the polluted output from resistant trivial solutions stuck in the standard version of the MPS is to introduce additional points in the interior of the scattering domain at which unadulterated solutions would then have a distinguishably larger norm. This control is due to the fact that only the more stable, unitary part from the QR decomposition of the extended matrix system is utilized in the final solution procedure. However, as Beyn's algorithm cannot be provided then any more, minimizers of certain singular values will serve as eigenvalue identifiers instead whose determination we will restrict to the real-valued case for simplicity. In contrast, as the general existence of transmission eigenvalues with non-vanishing imaginary part is still an open question, the latter simplification might be reasonably accepted. For recent investigations concerning the possible locality of ITEs, we refer to [45] and especially for spherically stratified media to [20, 16, 50, 18, 17].

The remainder of this paper is structured as follows: In section 2 we will introduce the interior transmission problem and derive its discretized MFS system to be investigated in section 3. There we show up the weak points of the standard MFS version and reproduce afterwards the successful extension from [5] for our framework

accompanied by positive numerical results. The corresponding approximation analysis will then be the focus of section 4. Finally, a conclusion will be given in section 5.

2. Problem statement

The acoustic interior transmission problem arises naturally as a special case of the more general scattering problem: Given an incident wave u_i and some homogeneous, penetrable 2D scattering object mathematically represented by a bounded domain $D \subset \mathbb{R}^2$ (which corresponds to an unbounded 3D scatterer with planar symmetry), the spatial transition of time harmonic waves is reflected by the following partial differential equation:

$$\Delta u + k^2 n u = 0 \quad \text{in } \mathbb{R}^2 \ . \tag{1}$$

Here, $n \neq 1$ denotes some positive dispersion-free index of refraction which is constant within D according to our modeling assumption and equal to unity in the exterior D^{c}, k is the wave number, and $u = u^i + u^s$ is the superposition of the incident wave, solving the Helmholtz equation in $\mathbb{R}^2$ modulo possible point source locations outside D, and its scattered response.

To obtain a physically plausible problem in which u represents an acoustic pressure fields, for instance, we impose the two dimensional Sommerfeld radiation condition

$$\lim_{r\to\infty} \sqrt{r}\,(\partial_r u^s - \mathrm{i}k u^s) = 0$$

which is to be understood uniformly in the angular direction and where $r = |x|$ is the radial component at position $x \in \mathbb{R}^2$. If not stated otherwise, $|\cdot|$ in combination with vectors in $\mathbb{C}^d$ for arbitrary dimension $d \in \{1, 2, 3, \ldots\}$ denotes the usual 2-norm throughout this paper. It is well known that the direct scattering problem of finding u is uniquely solvable, e.g. for $u \in H^1_{loc}(\mathbb{R}^2)$, see [14]. As usual, $H^m(\Omega)$ is the Sobolev space with respect to some open set Ω containing functions (which can additionally be assigned boundary data ($\sim H^m_0(\Omega)$) or be restricted to local integrability properties ($\sim H^m_{loc}(\Omega)$)) that are m times weakly differentiable with square integrable derivatives.

Closely related to the solvability of the associated inverse problem, but also interesting for its own is the question whether there exist incident waves u^i which do not scatter, i.e. we now seek for solutions satisfying $u^s = 0$ in D^{c}. A necessary criterion would be to find $w = u_{|D}$ and $v = u^i_{|D}$ which satisfy the so-called interior transmission problem (ITP): Determine $k \in \mathbb{C}\backslash\{0\}$ and non-trivial $v, w \in L^2(D)$ with $v - w \in H^2_0(D)$ solving in a distributional sense

$$\begin{aligned} \Delta w + k^2 n w &= 0 \quad \text{in } D \ , \\ \Delta v + k^2 v &= 0 \quad \text{in } D \ , \\ v &= w \quad \text{on } \partial D \ , \\ \partial_\nu v &= \partial_\nu w \quad \text{on } \partial D \ , \end{aligned} \tag{2}$$

where ν denotes the outer normal at the corresponding points of the boundary ∂D. Values of k fulfilling the above requirements are called interior transmission eigenvalues. However, the existence of transmission eigenvalues does generally not imply v to be extendible to all of $\mathbb{R}^2$ as a Helmholtz solution which then spoils the

interpretation of being a non-scattering incident field for (1). Even worse, in [8] the authors showed that for regions D with rectangular corners, interior transmission eigenvalues can never be such non-scattering numbers whose eigenfunctions extend globally.

A few words should also be noted about the regularity assumptions of (v, w): Since we now work with a boundary value problem, zero boundary data seem appropriate for the difference of $v \sim u^i_{|D}$ and $w \sim u_{|D}$. As a consequence, the intuitive attempt of interpreting (2) as a weak solution system in (v, w) in the usual componentwise $H^1(D)$-manner fails as this would result in a non-compact perturbation of an invertible operator which inhibits the application of Fredholm theory, for example. However, our particular assumption on the index of refraction being constant in D will then turn out to regularize v and w as elements in $H^2(D)$ as long as ∂D is smooth enough.

Concerning the computation of eigenvalues, the accuracy obtained from finite dimensional approximations can often be controlled in terms of some corresponding eigenfunction error, see for example [23] or Corollary 6 below. Consistency would then be linked to denseness properties of the approximation spaces. Due to our homogeneity assumption within D, (2) can equivalently be interpreted as a coupled Helmholtz system with interconnected wave numbers via the refractive index. In the context of the ITP the standard implementation of MFS based upon the so called "point-matching method" looks for radial basis functions divided into

$$V_m = \{\Phi_1, \dots, \Phi_m\} , \qquad W_m = \{\Psi_1, \dots, \Psi_m\} \tag{3}$$

such that for all $i = 1, \dots, m$, Φ_i and Ψ_i solve the Helmholtz equation exactly with wave number κ and $\sqrt{n}\kappa$, respectively. Furthermore, the latter factor relation makes it possible to correlate Φ_i and Ψ_i in a similar way and will even be implemented later. Given a set of boundary points $s_1, \dots, s_m \in \partial D$, we now make the ansatz for $1 \le i \le m$

$$v_m(s_i) = \sum_{j=1}^{m} c_j^{\Phi} \Phi_j(s_i) , \qquad w_m(s_i) = \sum_{j=1}^{m} c_j^{\Psi} \Psi_j(s_i) \tag{4}$$

and define the associated coefficient vector $c \in \mathbb{C}^{2m}$ by

$$c = (c_1^{\Phi}, \dots, c_m^{\Phi}, -c_1^{\Psi}, \dots, -c_m^{\Psi})^{\top} .$$

Next, we try to match the boundary conditions from (2) for all $i = 1, \dots, m$ in a non-trivial way:

$$\begin{aligned} v_m(s_i) &= w_m(s_i), \\ \partial_\nu v_m(s_i) &= \partial_\nu w_m(s_i). \end{aligned}$$

The solvability of this system of linear equations is equivalent to finding values of $\kappa \in \mathbb{C}\backslash\{0\}$ for which

$$T(\kappa) \equiv T_m(\kappa) := \begin{pmatrix} S_\Phi(\kappa) & S_\Psi(\kappa) \\ D_\Phi(\kappa) & D_\Psi(\kappa) \end{pmatrix} \tag{5}$$

is (approximately) singular. Here, the block matrix coefficients of $T(\kappa) \in \mathbb{C}^{2m \times 2m}$ are

given componentwise by

$$\begin{aligned}(S_\Phi(\kappa))_{i,j} &= \Phi_j(s_i)\ ,\\ (S_\Psi(\kappa))_{i,j} &= \Psi_j(s_i)\ ,\\ (D_\Phi(\kappa))_{i,j} &= \partial_\nu\Phi_j(s_i)\ ,\\ (D_\Psi(\kappa))_{i,j} &= \partial_\nu\Psi_j(s_i)\ ,\end{aligned}$$

with $1 \leq i, j \leq m$ and reflect the Dirichlet and Neumann boundary data from v_m and w_m, respectively. Finally, we interpret the derived system as the non-linear eigenvalue problem

$$T(\kappa)c = 0\ , \quad c \in \mathbb{C}^{2m}\backslash\{0\}\ , \quad \kappa \in \mathbb{C}\backslash\{0\} \tag{6}$$

and expect its solutions, or those κ giving a sufficiently small right-hand side in norm, to be close to some real interior transmission eigenvalue k from (2) for m large enough. We will denote both by k_m within this paper and call them approximate ITEs for now. Regarding the generation of T in detail, our basis functions from (3) will consist of two wave-number-dependent families of radiating fundamental solutions to the global Helmholtz equation, respectively. As convolution kernels, these consist of two symmetrically interchangeable variables and solve the targeted PDE when fixing one of them. Without loss of generality we will freeze the second variable, which we will call sources due to their delta-induced singularities and place them strictly outside of D on a sufficiently smooth closed curve Γ of finite Hausdorff measure. Finally selecting finitely many source points $\{y_j\}_{1\leq j\leq m} \subset \Gamma$ as parameters to obtain the desired family of linear independent Helmholtz solutions V_m and W_m, respectively, the resulting method solving (6) is called the MFS. An examplary setup may be seen in Figure 1.

According to our above derivation, this particular choice of trial functions is not the only one possible. But having in mind that solutions to the ITP might not be globally extendible across ∂D in general, our ansatz can reflect this curtailing behavior domain-independent and for free in polar form. Another advantage is that the eigenoperator T then becomes holomorphic and matrix-valued in the κ argument which enables us to apply a broader class of solution algorithms such as Beyn's algorithm.

3. Numerical Results

The MFS can be thought of as some discrete equivalent of an integral operator realization generated by a singular kernel which solves the Helmholtz equation. Indeed, let $\{K_\varkappa(\cdot, y)\}_{y\in\Gamma}$ be the 2D radiating fundamental solutions to the Helmholtz equation with sources on Γ and wave number $\varkappa$, i.e. $K_\varkappa(x, y) = H_0^{(1)}(\varkappa|x-y|)$ is the first Hankel function with $(\varkappa|x - y|)$-argument. Then, for any coefficient function $g \in L^2(\Gamma)$ the continuous superposition

$$[\hat{K}_\varkappa g](x) := \int_\Gamma K_\varkappa(x, y)g(y)\,\mathrm{d}y\ , \qquad x \in \overline{D} \tag{7}$$

also solves the same Helmholtz equation in D by linearity and equals the usual single layer potential on Γ. A natural discretization of the integral in (7) with respect to

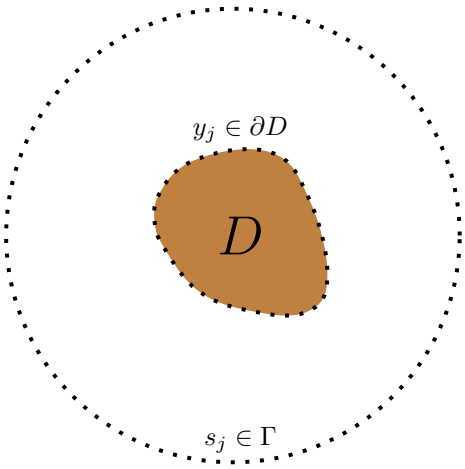

Figure 1. Examplary MFS setup: The dots represent the computational points of the scattering and the source boundary, respectively.

the sources y and choosing $\varkappa = \kappa, \sqrt{n}\kappa$, respectively, would finally result in linear combinations of the form (4), which was exactly our initial MFS ansatz.

An immediate drawback arising from this conceptional integral operator perspective is the following: Recall that in order to compensate finite precision arithmetics of computers, we slightly relaxed the term of an approximate ITE in the discrete setting (6) not to miss also rounded candidates giving sufficiently small non-zero boundary contributions. However, containing approximations of compact block operators $\hat{K}_\varkappa : L^2(\Gamma) \longrightarrow H^{\frac{3}{2}}(\partial D)$ or the corresponding Neumann modifications within T, these induce for each wave number $\varkappa$, or equivalently for each κ, a decreasing sequence of linear $T(\kappa)$-eigenvalues accumulating at zero when m tends to infinity. This fact is likely to hinder the numerical distinction between approximations of exact ITEs and arbitrary ones in disguise due to ill-conditioning in total. We will now discuss two different approaches for solving the non-linear eigenvalue problem (6) keeping that warning in mind. The first one, using Beyn's algorithm, will show the limiting effects of the underlying ill-conditioning with respect to the accuracy of the eigenvalue approximation accompanied by additional pollution already in the case of very simple scattering domains. In the subsequent section we will then see how to circumvent these issues using Betcke's & Trefethen's interior-points-extension.

3.1. Using Beyn's algorithm for the ITP

The first method we want to apply for solving (6) resulting from the MFS goes back to W.-J. Beyn in [6] and since then it was positively tested in the context of ITE computations using boundary integral equations in several papers such as in [36, 35, 15]. The main benefit is, especially compared to our second approach that will be presented in the next section, that the solution algorithm is more easily capable for finding eigenvalues from (6) with their multiplicities inside a prescribed contour located in the complex plane. The only relevant but restrictive condition for our cases is that it requires T to be holomorphic in z which is automatically fulfilled thanks to our MFS ansatz.

For convenience of the reader, we recall the main idea of Beyn's algorithm and refer to his original paper for further details: The starting point is a generalization of the Laurent series concept for scalar meromorphic functions to square matrix type thanks to Keldysh's theorem, see [42]. In this spirit, if $T(k_m) \in \mathbb{C}^{2m\times 2m}$ loses its full rank at some $k_m \in \mathbb{C}$ so that $T(\kappa)^{-1}$ becomes singular for $\kappa \longrightarrow k_m$, this blow-up should be reflected in the generation of certain poles at k_m. Indeed, in a small neighbourhood of any k_m fulfilling (6) exactly, we may write according to Keldysh

$$T^{-1}(\kappa) = R(z) + \sum_{i=-N(k_m)}^{-1} M_i(\kappa - k_m)^i \ ,$$

with $N(k_m) \in \mathbb{N}$, rank-one matrix coefficients $M_i \in \mathbb{C}^{2m\times 2m}$ such that $M_{-N(k_m)} \neq 0$ and R being a pure holomorphic matrix-valued function. In this way, the problem of finding approximate ITEs k_m is decoupled into a pole analysis for each component. Then, for any holomorphic function f, Cauchy's integral formula yields for a sufficiently close contour $\Gamma_{\mathbb{C}}$ around k_m

$$\frac{1}{2\pi \mathrm{i}} \int_{\Gamma_{\mathbb{C}}} f(\kappa) T^{-1}(\kappa)\, \mathrm{d}\kappa = \sum_{i=1}^{N(k_m)} \frac{f^{(i)}(k_m)}{i!} M_i \ .$$

It turns out that the above identity also holds for contours containing N different T^{-1}-poles $k_m^1, \ldots, k_m^N$ in analogy to the residue theorem so that we obtain in general

$$\frac{1}{2\pi \mathrm{i}} \int_{\Gamma_{\mathbb{C}}} f(\kappa) T^{-1}(\kappa)\, \mathrm{d}\kappa = \sum_{j=1}^{N} \sum_{i=1}^{N(k_m^j)} \frac{f^{(i)}(k_m^j)}{i!} M_i^j \ . \tag{8}$$

Since the values of k_m^j to be determined are now hidden in the implicit evaluation of proper functions f, Beyn suggests the choice of a monomial basis whose highest order depends on the number of T-eigenvalues inside of $\Gamma_{\mathbb{C}}$. Interpreting the resulting expressions as constant matrices (assembled as higher dimensional blocks in the most general case), systematic transformations including a singular value decomposition finally lead to a linear eigenvalue problem whose eigenvalues coincide with $k_m^1, \ldots, k_m^N$ including multiplicity encircled by $\Gamma_{\mathbb{C}}$.

Altogether, this procedure yields the guideline for Beyn's algorithm. From the numerical cost's perspective we thus need to compute primarily

(i) complex contour integrals including matrix inversions according to (8),

(ii) a singular value decomposition,

(iii) a linear eigenvalue problem.

While the integration given in item (i) needs to be performed for all components settled by the dimension of the non-linear eigenoperator T and the number of local T-eigenvalues, its componentwise computation requires only little work except for the explicit inversion of $T(\kappa) \in \mathbb{C}^{2m\times 2m}$ involved. For instance, the trapezoidal rule admits exponential convergence due to the contour-induced periodicity of the meromorphic integrands, implying the number of quadrature points to be uniformly limited. Concerning the solution of the final linear eigenvalue problem there are also no special difficulties so the common routines for matrices may be applied to recover the N distinct eigenvalues k_m^j. The most delicate step is the singular value

decomposition of an at least $(2m \times 2m)$-matrix, but its effective size depends on the frequency of locally enclosed T-eigenvalues that needs to be guessed. As a dimension reduction improvement, Beyn suggests a rank-maintaining right-multiplication of (8) with a rectangular random matrix. Similarly, an additional left-multiplication may be applied as it was positively checked in [15]. However, such simplifications increase the risk of a final rank drop and results in unexpected behavior of Beyn's algorithm in total.

In summary, this algorithm transforms a non-linear eigenvalue problem of the form (6) into a linear one and manages to compute local eigenvalues including muliplicity on the expense of controllable numerical utilities.

For now we have everything together to present first numerical ITE results based on the MFS combined with Beyn's algorithm. To warm up we would like to present our findings for the unit disc. This is an approved starting point as it is the easiest representative for arbitrary analytical 2D domains through the conformal mapping theorem, thus giving us a rough idea of what output quality could be generally expected. The block matrices of the eigenoperator (5) become with the extracted notation from (7), interpreting (2) as a Helmholtz system with wave numbers κ and $\sqrt{n}\kappa$, respectively

$$\begin{aligned} \left(S_\Phi(\kappa)\right)_{i,j} &= K_\kappa(s_i, y_j) \ , \\ \left(S_\Psi(\kappa)\right)_{i,j} &= K_{\sqrt{n}\kappa}(s_i, y_j) \ , \\ \left(D_\Phi(\kappa)\right)_{i,j} &= \partial_\nu K_\kappa(s_i, y_j) \ , \\ \left(D_\Psi(\kappa)\right)_{i,j} &= \partial_\nu K_{\sqrt{n}\kappa}(s_i, y_j) \ , \end{aligned} \tag{9}$$

where the normal derivative within the double layer kernels refer to the first argument each, i.e. with respect to s_i for $1 \leq i \leq m$. For simplicity of the second argument, we distribute $\{y_j\}_{1 \leq j \leq m} \subset \Gamma$ equidistantly on a circle with radius $R = 5$.

Fortunately, the simple geometry makes it possible to compute ITEs almost analytically by seeking for an exact Helmholtz solution pair (v, w) in polar coordinates (r, φ) of Fourier-Bessel form

$$v(r, \varphi) = c_p^v \sin(p\varphi) J_p(\kappa r) \ , \qquad w(r, \varphi) = c_p^w \sin(p\varphi) J_p(\sqrt{n}\kappa r) \tag{10}$$

where J_p denotes the Bessel function of the first kind with parameter $p \in \mathbb{N}_0$ and $c_p^v, c_p^w \in \mathbb{C}$. The fulfilment of ITP boundary conditions (2) for the unit disc $(r = 1)$ is then purely concentrated on the radial part of (10) and requires for a non-trivial solution (v, w) via c_p^v that

$$\det \begin{pmatrix} J_p(\kappa) & J_p(\sqrt{n}\kappa) \\ J_p'(\kappa) & \sqrt{n} J_p'(\sqrt{n}\kappa) \end{pmatrix} = 0$$

holds. In particular, fixing $n = 4$ and $p = 1$ as our benchmark values, one obtains $k \approx 2.902608055212766 \in \mathbb{R}$ as the real-valued root with smallest magnitude which is the ITE we now want to seek with our numerical computations. Figure 2 shows the output of the Beyn algorithm with MFS input and plots the absolute error measured with respect to k for an increasing number of collocation points.

More precise, our utilized Matlab routine successively incremented the iterations by 2 collocation points starting from $m = 5$ as no approximate eigenvalue was found for $m = 1, 3$ yet and filtered the value matching k best inside of the contour

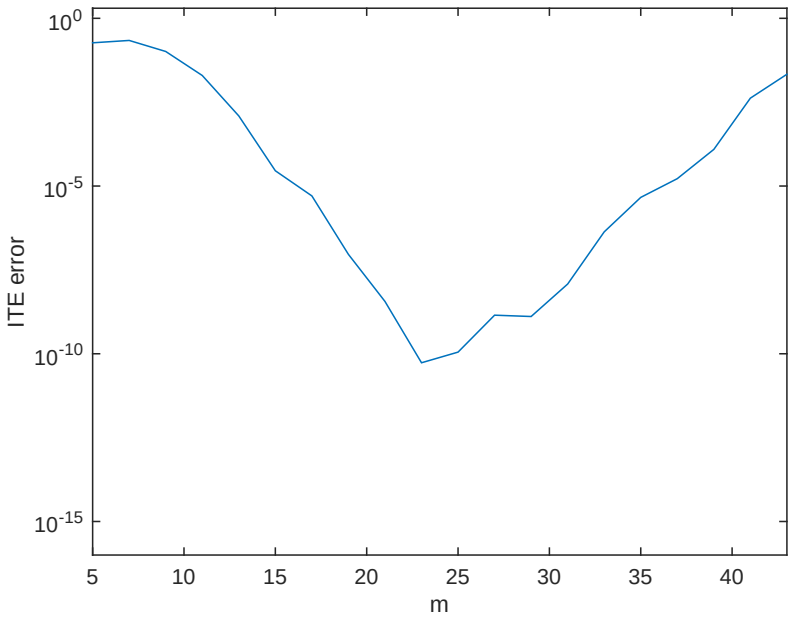

Figure 2. Absolute eigenvalue deviation from the smallest ITE of the unit disc computed with the standard MFS approach in combination with Beyn's algorithm.

$\Gamma_{\mathbb{C}} := \{3 + 0.5\mathrm{e}^{\mathrm{i}t}\}_{t\in[0,2\pi]}$ using double precision. The convergence history in Figure 2 shows that the decay is first supported by the increased number of collocation points to a minimum of about 10 correct digits, but is then fatally dominated by the blow-up of the condition number of the non-linear eigenoperator T locking any further gain in accuracy. Furthermore, additional pollution of pseudo-eigenvalues comes into play for larger values of m as foreseen at the beginning of the chapter, cf. Figure 3.

Our preliminary analysis indicates that we need an improvement of the standard MFS when applied in ITE studies to obtain reliable data, especially when working with more difficult domains D.

3.2. Using Betcke's & Trefethen's Algorithm for the ITP

From now on we will restrict to $\kappa \in \mathbb{R}_{>0}$ although our technique to be presented is also applicable in the complex case. We have previously seen that a crucial step in revealing real ITEs approximately under finite precision arithmetics is to filter spurious eigenvalues from the actual, but so far numerically-indistinguishable ones. As some positive remedy, Cossonnière, tackled by boundary integral methods, proposed in [21] to integrate the fact that there cannot be purely imaginary ITEs by considering a family of generalized linear eigenvalue problems instead which would read in our discrete MFS case, adapting (6) correspondingly

$$T(\kappa)c = \lambda T(\mathrm{i}\kappa)c, \quad c \in \mathbb{C}^{2m}\backslash\{0\},\ \kappa \in \mathbb{R}_{>0},\ \lambda \in \mathbb{C}\ .$$

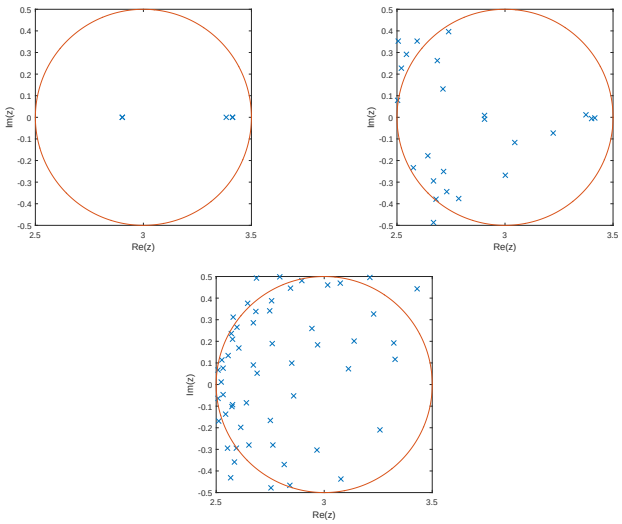

Figure 3. Pollution of the eigenvalue output: From left to right with $m = 20, 40, 60$, respectively, the three plots show how Beyn's algorithm in combination with the MFS produces spurious eigenvalues when approximating the smallest ITE of the unit disc within $\Gamma_{\mathbb{C}}$ under increasing number of collocation points.

In this way, the critical accumulation point with respect to λ is shifted from 0 to -1 whereas $\lambda = 0$ indicates $\kappa = k_m$ to be an approximate eigenvalue near a real ITE.

In the following, we want to introduce a different approach initiated by Betcke & Trefethen for screening spurious eigenvalues which is also applicable to other PDE-related eigenproblems. To understand the pollution from the abstract ITP perspective, we consider the inhomogeneous (boundary condition) version of (2)

$$\begin{aligned} \Delta\widetilde{w} + \widetilde{k}^2 n \widetilde{w} &= 0 \quad \text{in } D \ , \\ \Delta\widetilde{v} + \widetilde{k}^2 \widetilde{v} &= 0 \quad \text{in } D \ , \\ \widetilde{v} - \widetilde{w} &= \widetilde{f} \quad \text{on } \partial D \ , \\ \partial_\nu(\widetilde{v} - \widetilde{w}) &= \widetilde{g} \quad \text{on } \partial D \ , \end{aligned} \tag{11}$$

where $\widetilde{v}, \widetilde{w} \in L^2(D)$, $\widetilde{v} - \widetilde{w} \in H^2(D)$, $\widetilde{f} \in H^{\frac{3}{2}}(\partial D)$ and $\widetilde{g} \in H^{\frac{1}{2}}(\partial D)$. Then, it can be shown, see [12], that there is a constant $\widetilde{C}$ depending only on $\widetilde{k}$ and D such that

$$\|\widetilde{v}\|_{L^2(D)} + \|\widetilde{w}\|_{L^2(D)} \leq \widetilde{C} \left(\|\widetilde{f}\|_{H^{\frac{3}{2}}(\partial D)} + \|\widetilde{g}\|_{H^{\frac{1}{2}}(\partial D)} \right) \ ,$$

provided $\widetilde{k}$ is not an interior transmission eigenvalue. Although $\widetilde{C}$ blows up for $\widetilde{k} \longrightarrow k$, by fixing some value unequal to any ITE this estimate clearly shows that small boundary contributions imply small interior norm of the $\widetilde{k}$-associated pair $(\widetilde{v}, \widetilde{w})$. As a consequence, since T in (6) captures only the boundary parts of our trial functions, spurious eigenvalues just arise as unintended global approximations of $\widetilde{v} = \widetilde{w} = 0$ in $\overline{D}$ that need to be excluded within our computations.

Therefore, we want to include the information of the eigenfunction's interior behavior and extend the collection of m boundary collocation points $\{s_i\}_{1 \leq i \leq m}$ on

∂D by $m_I = \text{const}$ additional points $\{x_i\}_{1\le i\le m_I}$ inside of D and likewise the block matrix T from (5) to

$$\widetilde{T}(\kappa) := \begin{pmatrix} S_\Phi(\kappa) & S_\Psi(\kappa) \\ D_\Phi(\kappa) & D_\Psi(\kappa) \\ S_\Phi^I(\kappa) & 0 \\ 0 & S_\Psi^I(\kappa) \end{pmatrix} \in \mathbb{C}^{(2m+2m_I)\times 2m} \ . \tag{12}$$

The structure of the appended $S_\bullet^I$-blocks is equal to those of the first line but now evaluated at the m_I interior points instead of at $\{s_i\}_{1\le i\le m}$ in (9). In order to quantify a numerically robust filter that seeks for approximate eigenfunctions with small boundary parts but relatively large interior contribution, we take over the cleverly-integrated QR manipulation of Betcke & Trefethen proposed in [5]: Writing

$$\widetilde{T}(\kappa) = \widetilde{Q}(\kappa)\widetilde{R}(\kappa) = \begin{pmatrix} Q(\kappa) \\ Q_I(\kappa) \end{pmatrix} \widetilde{R}(\kappa) \ , \quad \text{with } \widetilde{R}(\kappa), Q(\kappa) \in \mathbb{C}^{2m\times 2m}$$

we immediately see that $\mathrm{Im}T(\kappa) = \mathrm{Im}Q(\kappa)$ provided $\widetilde{R}(\kappa)$ is unconditionally invertible. The latter is a reasonable assumption since we believe in choosing m_I so large to exclude the overall possibility of non-trivial solutions to (11) that vanish inside of D at that many points (note $\widetilde{R}(\kappa)c = 0$ implies $\widetilde{T}(\kappa)c = 0$). Therefore, any element q in the range of $Q(\kappa)$, or equivalently $\widetilde{q} \in \widetilde{Q}(\kappa)$ with $\widetilde{q}_{|\mathbb{C}^{2m}} = q$, can be identified with a pair (v_m, w_m) from (4) evaluated at our total $(m + m_I)$ points via a proper coefficient vector c and there exists $r \in \mathbb{C}^{2m}$ such that $\widetilde{q} = \widetilde{Q}(\kappa)r$. Keeping in mind the task of minimizing the boundary-misfit-to-interior ratio, these algebraic observations enable us to turn the non-linear eigenvalue problem from (6) into a searching procedure for (almost) vanishing $|q|$-magnitudes of $\widetilde{q} \in \widetilde{Q}(\kappa)$ constrained to $|\widetilde{q}| = 1$. Since $|\widetilde{q}| = 1 \Leftrightarrow |\widetilde{r}| = 1$, this can be further shifted to a local minimization in κ for the smallest singular value from the truncated boundary part $Q(\kappa)$ and reads in compact form

$$\text{Minimize} \qquad \kappa \longmapsto \min_{r\in\mathbb{C}^{2m},|r|=1} |Q(\kappa)r| \equiv \sigma_{\min}(Q(\kappa)) \ , \qquad \kappa \in U \subset \mathbb{R}_{>0} \ . \tag{13}$$

Again, we will call those arguments $\kappa = k_m$ giving sufficiently small minima in (13) approximate ITEs according to the identification

$$\begin{aligned} &\sigma_{\min}(Q(k_m)) = |\widetilde{Q}(\kappa)r_m| = |(\widetilde{Q}(\kappa)\widetilde{R}(\kappa))(\widetilde{R}(\kappa)^{-1}r_m)| = |\tilde{T}(\kappa)(\widetilde{R}(\kappa)^{-1}r_m)| \\ =&\sqrt{\sum_{i=1}^{m}(v_m(s_i) - w_m(s_i))^2 + (\partial_\nu(v_m(s_i) - w_m(s_i)))^2} \end{aligned} \tag{14}$$

with the obvious r_m-realization for (v_m, w_m). The sets U are introduced to isolate contributions from distinct k_m when m is fixed. At this point, note that the QR-improvement by Betcke & Trefethen is incompatible with Beyn's algorithm as the derived unitary part $\widetilde{Q}$ of any holomorphic matrix-valued function is not holomorphic any more in κ according to its global boundedness of each component prohibited by Liouville's well-known theorem from complex analysis unless $\widetilde{Q}$ is already constant. Still our $\widetilde{Q}$-based reformulation of the original problem (6) will provide us now with two major numerical advantages:

First, if k_m is an approximate ITE such that $\sigma_{\min}(Q(k_m))$ is small, the following calculation yields with the notation from (14)

$$\begin{aligned}&\sum_{i=1}^{m_I}|v_m(x_i)|^2+\sum_{i=1}^{m_I}|w_m(x_i)|^2=|T(k_m)(\widetilde{R}(k_m)^{-1}r_m)|^2\\ =&|Q_I(k_m)\widetilde{R}(k_m)\widetilde{R}(k_m)^{-1}r_m|^2=|Q_I(k_m)r_m|^2\\ =&|\widetilde{Q}(k_m)r_m|^2-|Q(k_m)r_m|^2=1-\sigma_{\min}(Q(k_m))^2\approx 1\ .\end{aligned}\tag{15}$$

Consequently, k_m claims (v_m, w_m) to be significantly large in the interior and effectively excludes its possibility of being a spurious approximate eigenvalue. Conversely, the inclusion of candidates with small pointwise interior norm which was the main cause for pollution in the old verion of MFS would now be penalized by large boundary contributions and thus not be favoured within (13) at all.

Second, we shall show that if some κ is distant from any ITE with $\sigma_{\min}(Q(\kappa))\gg 0$ in exact arithmetic, then our updated MFS version is able to reject this undesired sample as such numerically. Therefore, we want to show that the condition number of $Q(\kappa)$ stays harmless which follows easily from the fact that $\|\!|Q(\kappa)^{-1}|\!\| = \frac{1}{\sigma_{\min}(Q(\kappa))}$ being relatively bounded by assumption and $\|\!|Q(\kappa)|\!\| \leq \|\!|\widetilde{Q}(\kappa)|\!\| = 1$, where $\|\!|\cdot|\!\|$ denotes the spectral norm for matrices induced by $|\cdot|$. We can even enforce $\sigma_{\min}(Q(\kappa))$ in the considered regime to become nearly unity after multiplying the interior blocks $S^I_\bullet$ by a small number within $\widetilde{T}(\kappa)$. This sometimes has the advantageous secondary effect of globally polarizing the graph of $\kappa\mapsto\sigma_{\min}(Q(\kappa))$ in (13) stronger as being almost zero for approximate eigenvalues and close to unity otherwise. The latter constancy comes from the fact that all singular values will be lifted due to the less weighting of the interior part while being uniformly bounded from above by 1.

Remark 1. *Note that in practice the system for computing c when $\sigma_{min}(Q(\kappa))\approx 0$ is still very ill-conditioned. A numerically more stable but related procedure was later suggested by Betcke in [4] for recovering the corresponding approximate eigenfunctions. Likewise, the method can also be used for computing k_m in* (13) *by minimizing smallest generalized singular values instead which, however, does not show any advantage here.*

Altogether, our [5]-inspired MFS-adaption, which we will now refer to as extended or modified MFS, indeed serves as a filter for extracting unbiased approximate ITEs, at least from a theoretical point of view so far. To convince ourselves from the practical benefit of this method, we present our results for the unit disc re-chasing $k\approx 2.902608055212766$ with varying m but fixed $m_I=10$. Concerning the location of the computational points involved, we distributed the corresponding ones for the boundary, the interior and the sources equidistantly on a circle with radius 1, 0.5 and 5, respectively. Unlike in our first attempt, Figure 4 clearly shows that the recent approach is more stable when increasing the number m of boundary collocation points and manages to approximate k for the unit disc up to machine precision. Again, we used a Matlab routine for the ITE calculation with (+2)-increment for the iteration within the plotted m-range and employed the specific function *fminsearch* with optimization flag *optimset('TolX',1e-16)* as minimization tool. Repeating this procedure for successively higher singular values σ_i in (13) instead of only for the smallest one, the modified MFS shall also reveal the eigenvalue's multiplicity by counting identical minima in the wave number with respect to different singular values. This is because singular vectors to different but sufficiently small σ_i, whose magnitude

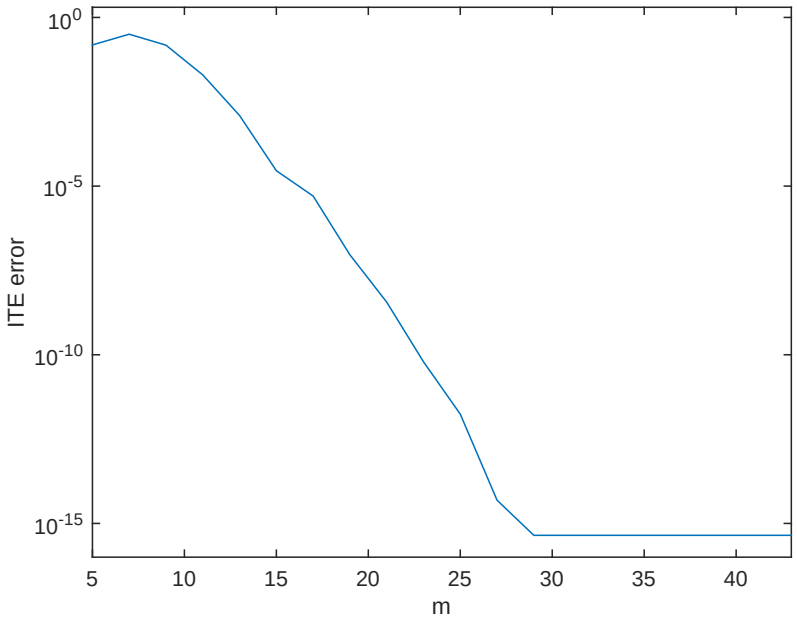

Figure 4. Absolute eigenvalue deviation with exponential decay from the smallest ITE of the unit disc computed with the extended MFS.

still measures the boundary misfit similar to (14), correspond to linear independent approximate eigenfunctions. According to this observation and Figure 5, we believe, for instance, that the three smallest ITEs for the unit disc have multiplicity 2,1,2 in increasing order, respectively. Apparently, Beyn's algorithm is definitely superior to the singular-value-based output in this aspect as the predicted multiplicity information is automatically released then.

In order to get a feeling about how the extended MFS reacts to other popular domains, we compare a family of consecutive shape deformations in the sequel and explore their effects on the ITE approximation accuracy. First we want to focus on the transition from a disc to several ellipses where we keep the major semi-axis fixed as one and shrink the minor semi-axis step by step. For this we selected m equiangular collocation points along the scattering boundary whereas the complementing source points were distributed equidistantly on a circle with radius 5. The main code we used for producing the ITE approximations was else - and in what follows will be - the same as for the unit disc above under the modified MFS. The final output is displayed in Figure 6: The determined values rely on a stable confidence regime for those approximate ITEs associated to sufficiently large m for which the minimal singular value in (13) was at least of order 10^{-10}. If any tail-digit is put in brackets, this indicates the existence of minor outliers within the computation obeying mostly the acceptance threshold though. Obviously, the varying number of correct digits, which we limited to a maximum of 15 in total due to possible round-off errors affecting the last digit of double-precision numbers, suggests that the less a domain deviates from the reference disc, the better the achievable accuracy of our computational ITE

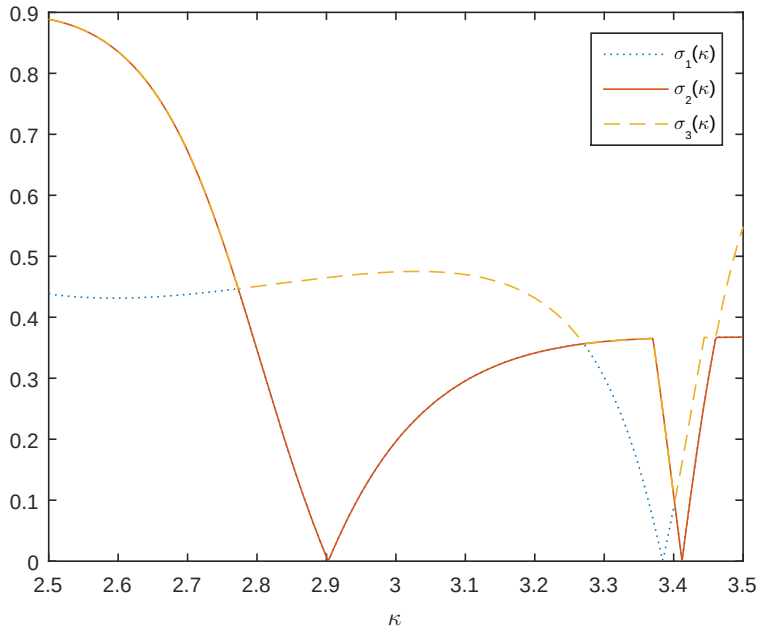

Figure 5. The graphs shows the first three smallest singular values of $Q(\kappa)$ including multiplicities for the unit disc with $m = 30$ collocation points. For example, the local minimum around the smallest approximate ITE clearly disappears for the third singular value which indicates that its eigenvalue multiplicity is two.

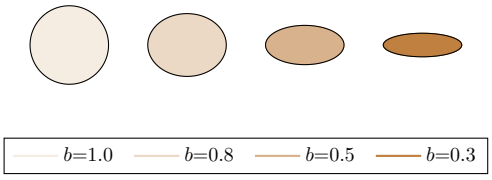

Shape	**Specifier**	**ITE 1**	**ITE 2**	**ITE 3**	**ITE 4**
Ellipse (disc)	semi axis=1	2.90260805521276	3.38419483954017	3.41205395159979	3.97647211159188
Ellipse	semi axis=0.8	3.13534121519068	3.48518298654316	3.54733071042719	3.88430612796681
Ellipse	semi axis=0.5	4.33068623074(1)	4.36895654200(3)	5.40918291160(8)	5.60124857917
Ellipse	semi axis=0.3	6.552756364(5)	6.56055364(1)	8.0949566	8.1574357

Figure 6. First four approximate real-valued ITEs for ellipses with unitary major semi-axis based on the modified MFS without multiplicity with $n = 4$. Digits given in brackets underlay computational fluctuations but are expected to be correct as well.

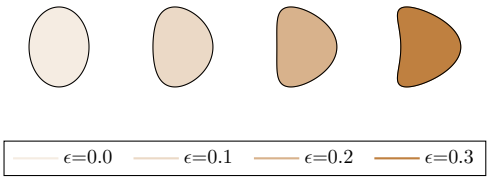

Shape	**Specifier**	**ITE 1**	**ITE 2**	**ITE 3**	**ITE 4**
Deformed ellipse	$\epsilon = 0.0$	3.235703038847477	3.611128205541419	3.691028926072422	4.058250609789813
Deformed ellipse	$\epsilon = 0.1$	3.2763480279118	3.5945609393239	3.73942279460228	4.07208521966683
Deformed ellipse	$\epsilon = 0.2$	3.38239714(4)	3.61769602(6)	3.807719411(8)	4.127129460(5)
Deformed ellipse	$\epsilon = 0.3$	3.51642(2)	3.69403(2)	3.87530(5)	4.21836(6)

Figure 7. First four approximate real-valued ITEs for deformed ellipses based on the modified MFS without multiplicity with $n = 4$. Digits given in brackets underlay computational fluctuations but are expected to be correct as well.

output becomes. The same observation was also made in the next experiment, where an ellipse with a semi-axes ratio of 0.75 was successively deformed to a kite shape and whose parametrizations obey

$$t \mapsto (0.75\cos(t) + \epsilon\cos(2t), \sin(t)) \ , \quad 0 \leq t < 2\pi \ .$$

Actually, this family of scatterers was introduced in [15] for ITE recovery under boundary integral methods which we may therefore use as further benchmark values, too. The modified MFS responds to those domains in terms of the perturbation parameter ϵ and equipped with equiangular boundary points according to Figure 7: While the location of source points only played a minor role regarding the approximation quality for the stretched ellipses, it really matters here, where a radius of 2 seems to be quite optimal when restricting Γ to concentric circles around the deformed ellipses. In the context of pure Helmholtz boundary value problems and smooth domains, see [3], the authors showed that convergence rates of the MFS depend on how far eigenfunctions can be analytically continued over D which might serve as a rule of thumb also in our ITE framework via the embracing radius of the source points. However, we neither tried to optimize the forming of Γ further nor exploited symmetries of the scatterers towards accuracy improvements as the results gained so far proved the extended MFS to be more than competitive with the standard methods for calculating ITEs. In particular, we were able to improve the results given in [15].

The situation gets worse if we consider non-smooth domains with corners, for example regular polygons. Here, we were only able to extract about 4 decimal places each with occasional individual improvements although we believe that the accuracy augments again for sufficiently many corners since then the unit disc is approximated. Our final results are listed in Figure 8 for polygonal edges of unit length each. They were obtained by equidistant computational points without touching any corners and

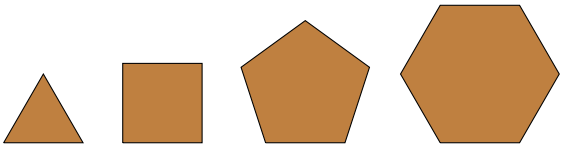

Shape	**ITE 1**	**ITE 2**	**ITE 3**	**ITE 4**
Triangle	8.9666(38)	9.40511(3)	10.54934(3)	12.43355(8)
Square	5.47610(8)	6.10028(3)	6.18437(4)	6.65095(0)
Pentagon	4.0556(0)	4.6715(5)	4.7198	5.5188(4)
Hexagon	3.2562(0)	3.7745(4)	3.8132(2)	4.3429(6)

Figure 8. First four approximate real-valued ITEs for the first four regular polygons based on the modified MFS without multiplicity with $n = 4$. Digits given in brackets underlay computational fluctuations but are expected to be correct as well.

with Γ as the circumference scaled with a factor of 1.5 away from the scattering boundary.

The loss of accuracy may be explained here by the quintessence of [8] that eigenfunctions cannot be locally extended around corners of D at all. While we already chose the source point as artificial singularities relatively close to the polygons in this spirit, Γ is on the other hand constrained to lie disjoint around ∂D by the discretized MFS formulation to avoid poles along the scattering boundary (deteriorating the well-posedness of Dirichlet and Neumann data otherwise). Recently, an even more concrete behavior of the eigenfunctions near singular points was given in [7].

Summing up, convergence rates in m apparently correlate with continuation properties across ∂D of the eigenfunctions whose ITEs we try to approximate. Likewise, but more obvious in terms of the singular value, the speed of convergence with respect to the number of collocation points needed to reach the domain-specific exactness seems to be controlled in terms of its complexity (e.g. m was typically larger than 50 for the polygons to guarantee a significant accumulation of the computed ITEs whereas the convergence history up to $m = 40$ was sufficient for the scaled ellipses). While being sensitive for the boundary-related parameters, the MFS' output hardly shows any relevant dependency on the interior points which were therefore distributed throughout on circles that are fully contained in the scatterer. Altogether, despite its simple implementation, the modified MFS proved to be a very powerful and beneficial alternative for ITE approximations whose weak points merely emerge in combination with angled or too advanced domains.

In the next section, we want to provide an ITP-specific theoretical framework for the modified MFS analysis and give some natural relation between $\sigma_{min}(Q(k_m))$ and the deviation of approximate eigenvalues k_m from the nearest exact one that was our implicitly-believed guideline when generating our tables above.

4. Approximation analysis

As we want to investigate in what results could be expected in a limiting process $m \longrightarrow \infty$ with respect to our computed approximate eigenfunctions (v_m, v_m) from the modified MFS, we now turn our attention to the broader, continuous setting of function spaces in the following and try to assimilate the discrete perspective thereby. Regularity assumptions on ∂D and Γ will play a crucial role since we now want to

control the behavior of the eigenfunctions along the total boundary instead of only at m selected sample points. In what follows, $C^\ell(D)$ will denote, as usual, the classical space of functions on D being ℓ times continuously differentiable with $m \in \mathbb{N}$ and $C^\infty(D) := \bigcap_{\ell\in\mathbb{N}} C^\ell(D)$. For getting a feeling in which function space our solutions to be approximated could be, we state the following lemma and develop a proper candidate space setup for the eigenfunctions afterwards. The crucial observation regarding the ITP is that while the coupled system is non-elliptic (in the sense of Agmon-Douglis-Nirenberg) in v and w, the difference $v-w$ solves a fourth order scalar elliptic equation which regularizes the problem for smooth domains and refractive indices.

Lemma 1. *Let ∂D be of class C^4 (i.e. $\overline{D}$ is a C^4-manifold with boundary ∂D embedded in $\mathbb{R}^2$) and let (v, w) be a solution to (2) with $n_{|D} \in \mathbb{R}\backslash\{1\}$ for some interior transmission eigenvalue $k > 0$. Then $v, w \in H^2(D) \cap C^\infty(D)$.*

Proof. We set $f := w - v$ and verify the identities

$$v = -\frac{\Delta f + k^2 n f}{k^2(n-1)} \qquad \text{and} \qquad w = -\frac{\Delta f + k^2 f}{k^2(n-1)} \ .$$

Therefore, the assertion follows if we can show that $f \in H^4(D)\cap C^\infty(D)$. Fortunately, $f \in H_0^2(D)$ itself solves the (uniformly strongly) fourth order elliptic equation with constant coefficients

$$\Delta^2 f + k^2(n+1)\Delta f + k^4 n f = 0 \quad \text{in } D$$

in a weak sense. Applying global elliptic regularity theory of general order, see [1] for example, we may conclude that indeed $f \in H^4(D)$ due to the smoothness assumption on ∂D as well as $f \in H^\ell(D')$ for every $\ell \in \mathbb{N}$ and for all compactly contained $D' \subset\subset D$ according to elliptic interior improvements which finally implies $v, w, f \in C^\infty(D)$ by the Sobolev Embedding Theorem. □

From now on we assume that ∂D is of class C^4, $n_{|D} \in \mathbb{R}\backslash\{1\}$ and $k > 0$. Since interior transmission eigenfunctions are then actually in $H^2(D) \times H^2(D)$ instead of only distributional solutions according to the above lemma, this encourages to define the relaxed function space $\mathcal{H}$ by

$$\mathcal{H} := \bigcup_{\kappa\in\mathbb{R}_{>0}} \mathcal{H}(\kappa) \ ,$$

where

$$\mathcal{H}(\kappa) := \mathcal{A}(\kappa) \times \mathcal{A}(\sqrt{n}\kappa)$$

and

$$\mathcal{A}(\varkappa) = \{h \in H^2(D) \cap C^\infty(D) : \Delta h + \varkappa^2 h = 0\} \ .$$

By comparing with the block matrix structure in (12), we see that $\widetilde{T}(\kappa)$ reflects in its first two block lines the pointwise deviation of coupled Dirichlet and Neumann boundary data and then individually the evaluation at shared inner points, respectively. From this point of view, $\widetilde{T}(\kappa)$ may be considered as a measure for the

quality of approximate eigenfunctions in the pointwise sense. In analogy, we may now endow each $\mathcal{H}(\kappa)$ with the inner product (although we will not work with it as such since we will rather treat the summands according to the offset below as induced norms separately due to their opposed roles)

$$\begin{aligned}(a,b)_{\mathcal{H}} :=&(a_1-a_2,b_1-b_2)_{H^{\frac{3}{2}}(\partial D)}+(\partial_\nu(a_1-a_2),\partial_\nu(b_1-b_2))_{H^{\frac{1}{2}}(\partial D)}\\ &+(a_1,b_1)_{L^2(D)}+(a_2,b_2)_{L^2(D)}\end{aligned} \tag{16}$$

using the abbreviations $a=(a_1,a_2)\in\mathcal{H}(\kappa)$ and $b=(b_1,b_2)\in\mathcal{H}(\kappa)$. Theorem 2 below will show that the specific fractional Sobolev exponents within the boundary parts of the inner product are the appropriate ones in order to extend the boundary difference traces of any approximate eigenvector pair to a more convenient error function on D whose interior norm is still proportionally small. Apart from that, presuming an unobstructed conversion from our finite dimensional measurements to $\|\cdot\|_{\mathcal{H}}$, we can now prove feasibility of the extended MFS embedded in the space $\mathcal{H}$ for ITE approximations freed from eigenvalue pollution and discuss afterwards how to justify the transitional assumptions.

Theorem 2. *Assume* $\{(v_m,w_m,k_m)\}_{m\in\mathbb{N}}\subset\mathcal{H}\times\mathbb{R}_{>0}$ *and* $\{(\theta_m^D,\theta_m^N)\}_{m\in\mathbb{N}}\subset H^{\frac{3}{2}}(\partial D)\times H^{\frac{1}{2}}(\partial D)$ *are such that the following conditions hold:*

(i) eigenvalue convergence: $k_m\longrightarrow k$ *,*

(ii) uniform interior bound: $C^{-1}<\left(\|v_m\|^2_{L^2(D)}+\|w_m\|^2_{L^2(D)}\right)<C$ *for some* $C>1$ *and for all* m *large enough,*

(iii) approximate ITP: $(\widetilde{v},\widetilde{w},\widetilde{f},\widetilde{g},\widetilde{k})=(v_m,w_m,\theta_m^D,\theta_m^N,k_m)$ *is a solution of* (11) *for all* m *large enough with identical refractive index* $n>0$ *and asymptotically vanishing boundary data* $\left(\|\theta_m^D\|_{H^{\frac{3}{2}}(\partial D)}+\|\theta_m^N\|_{H^{\frac{1}{2}}(\partial D)}\right)\longrightarrow 0$ *with respect to* m*.*

Then, there exists a distributional solution $(v,w)\in\mathcal{H}$ *of* (2) *with interior transmission eigenvalue* k*.*

Proof. We aim to bound $\|v_m-w_m\|_{H^2(D)}$ uniformly in m to extract a weakly convergent subsequence of $\{(v_m,w_m)\}_{m\in\mathbb{N}}$ with correctly coupled boundary data whose limit is then our solution candidate.

Indeed, weak $L^2(D)$-compactness directly yields (modulo subsequences which we will not relabel in m) that $v_m\rightharpoonup v$ and $w_m\rightharpoonup w$ in $L^2(D)$ thanks to our uniform bounds from (ii). Furthermore, v and w are distributional solutions to the Helmholtz equation with wave number k and $\sqrt{n}k$, respectively, since for all smooth and compactly supported φ in D we have by the third assumption

$$\begin{aligned}\int_D v(\Delta\varphi+k^2\varphi)\,\mathrm{d}x&=\lim_{m\to\infty}\int_D v_m(\Delta\varphi+k_m^2\varphi)\,\mathrm{d}x\\ &=\lim_{m\to\infty}\int_D\varphi\,\underbrace{(\Delta v_m+k_m^2v_m)}_{=0}\,\mathrm{d}x=0\ .\end{aligned}$$

The same calculation with adapted wave number holds true for w so we are left to prove that $(v-w)\in H_0^2(D)$ and $(v,w)\neq 0$:

Let us now bound $\|v_m - w_m\|_{H^2(D)}$. According to [41], for every m there exists a lifting function $\theta_m \in H^2(D)$ such that $\theta_{m|\partial D} = \theta_m^D$, $\partial_\nu \theta_{m|\partial D} = \theta_m^N$ and

$$\|\theta_m\|_{H^2(D)} \leq c\Big(\|\theta_m^D\|_{H^{\frac{3}{2}}(\partial D)} + \|\theta_m^N\|_{H^{\frac{1}{2}}(\partial D)}\Big) \tag{17}$$

for some $c > 0$. The triangle inequality shows

$$\begin{aligned}
&\|v_m - w_m\|_{H^2(D)} \\
\leq &\|v_m - w_m - \theta_m\|_{H^2(D)} + \|\theta_m\|_{H^2(D)} \\
\leq &\|v_m - w_m - \theta_m\|_{H_0^2(D)} + c\Big(\|\theta_m^D\|_{H^{\frac{3}{2}}(\partial D)} + \|\theta_m^N\|_{H^{\frac{1}{2}}(\partial D)}\Big)
\end{aligned}$$

and it remains to find an upper threshold for the first summand due to assumption (iii). However, since for all $u \in H_0^2(D)$ and some domain specific constant $\widetilde{c} > 0$ it holds that $\|u\|_{H_0^2(D)} \leq \widetilde{c}\|\Delta u\|_{L^2(D)}$ by elliptic a priori estimates, see [25], it suffices to bound $\|\Delta(v_m - w_m - \theta_m)\|_{L^2(D)}$ uniformly in m. Fortunately, v_m and w_m fulfill the Helmholtz equation exactly with wave numbers k_m and $\sqrt{n}k_m$, respectively, so the Laplacian can be easily controlled by

$$\begin{aligned}
&\|\Delta(v_m - w_m - \theta_m)\|_{L^2(D)} \\
\leq &\|\Delta v_m\|_{L^2(D)} + \|\Delta w_m\|_{L^2(D)} + \|\Delta \theta_m\|_{L^2(D)} \\
\leq &k_m\|v_m\|_{L^2(D)} + nk_m\|w_m\|_{L^2(D)} + c\Big(\|\theta_m^D\|_{H^{\frac{3}{2}}(\partial D)} + \|\theta_m^N\|_{H^{\frac{1}{2}}(\partial D)}\Big) \\
\leq &(\sup_m |k_m|)(\max\{n,1\})\sqrt{C} + c\Big(\sup_m \Big(\|\theta_m^D\|_{H^{\frac{3}{2}}(\partial D)} + \|\theta_m^N\|_{H^{\frac{1}{2}}(\partial D)}\Big)\Big) < \infty\ .
\end{aligned}$$

In the last line, we utilized all bounding assumptions from our theorem and have altogether shown that $\sup_m \|v_m - w_m\|_{H^2(D)} < \infty$. Therefore, we have (taking a further subsequence in m) that $(v_m - w_m) \rightharpoonup d^*$ in $H^2(D)$. By assumption (iii) in combination with (17) we thus conclude that the weak limit of $(v_m - w_m)$ in $H^2(D)$ and that of $(v_m - w_m - \theta_m)$ in $H_0^2(D)$ coincide, so that we actually have $d^* \in H_0^2(D)$. By linearity we also know that $(v_m - w_m) \rightharpoonup (v - w)$ in $L^2(D)$ and uniqueness of corresponding weak limits finally implies $d^* = (v - w) \in H_0^2(D)$.

It remains to show that $(v, w) \neq 0$. For this we use the fact that the embedding $H^2(D) \hookrightarrow H^1(D)$ is compact which implies $(v_m - w_m) \longrightarrow (v - w)$ strongly in $H^1(D)$ and in particular with respect to $L^2(D)$. Having this in mind we observe that (v, w) would be a non-trivial solution of (2) with ITE k if $\|v - w\|_{L^2(D)} > 0$. Therefore we assume contrarily that $(v_m - w_m) \longrightarrow 0$ in $L^2(D)$. Since the ITP consists of linear PDEs with real-valued eigenvalues under consideration, we may continue with either the real or imaginary parts of (v_m, w_m) without relabeling them such that condition (ii) is still fulfilled (with a possibly larger constant C). Then our artificial assumption yields

$$\liminf_{m\to\infty} (v_m, w_m)_{L^2(D)} = \liminf_{m\to\infty} \frac{\|v_m\|_{L^2(D)}^2 + \|w_m\|_{L^2(D)}^2}{2} \geq \frac{1}{2C} > 0\ .$$

Note that we cannot transfer this lower bound to (v, w) as $\{(v_m, w_m)\}_{m\in\mathbb{N}}$ converges only weakly. The desired contradiction still arises by applying Green's formula twice

and incorporating (the real part of) the lifting function from above again in the form

$$\begin{aligned}
0 \neq & \liminf_{m\to\infty} k^2(1-n)(v_m, w_m)_{L^2(D)} \\
&= \liminf_{m\to\infty} \int_D w_m \Delta v_m - v_m \Delta w_m \,\mathrm{d}x \\
&= \liminf_{m\to\infty} \int_{\partial D} w_m \partial_\nu v_m - v_m \partial_\nu w_m \,\mathrm{d}s \\
&= \liminf_{m\to\infty} \int_{\partial D} w_m \partial_\nu (v_m - w_m) - (v_m - w_m)\partial_\nu w_m \,\mathrm{d}s \\
&= \liminf_{m\to\infty} \int_{\partial D} w_m \partial_\nu \theta_m - \theta_m \partial_\nu w_m \,\mathrm{d}s \\
&= \liminf_{m\to\infty} \int_D \theta_m \Delta v_m - v_m \Delta \theta_m \,\mathrm{d}x \\
&= \liminf_{m\to\infty} \int_D \theta_m (-k_m^2 v_m) - v_m \Delta \theta_m \,\mathrm{d}x \\
&= \liminf_{m\to\infty} \int_D v_m (-k_m^2 \theta_m - \Delta \theta_m) \,\mathrm{d}x \\
&= 0 \ ,
\end{aligned}$$

where the last equality follows from (17), (*iii*) and

$$\left| \int_D v_m (-k_m^2 \theta_m - \Delta \theta_m) \,\mathrm{d}x \right| \leq \sup_m \{1, |k_m^2|\} \underbrace{\|v_m\|_{L^2(D)}}_{\leq C} \|\theta_m\|_{H^2(D)} \longrightarrow 0 \ .$$

□

Comparing with the concrete information provided by our practically implemented version of the modified MFS when neglecting minor discretization effects, we see that assumptions $(i) - (iii)$ of Theorem 2 can be reasonably checked during the computational procedure: The triple sequence $\{(v_m, w_m, k_m)\}_{m\in\mathbb{N}}$ arises as realizations of (14), so the first question whether the calculated $\{k_m\}$ are Cauchy or not can be answered by inspection of the programme's output. Next, (*ii*) is a consequence of (15). However, we did not state this condition in an almost equality form within the theorem's requisites although the latter reference might suggest that we have unit interior norm control apart from a small tolerance associated to the vanishing pointwise boundary misfit. The reason for our weaker formulation is that it is only the finite dimensional Euclidean norm giving that sharp QR-based lower bound for the inner points which needs to be coherently adopted to the governing continuous setting. Therefore, we demand that m_I is large enough but fixed to have a better chance of obtaining also a derived interior control with respect to $\|\cdot\|_{L^2(D)}$ for (v_m, w_m) as necessarily demanded by the uniform bounds from (*ii*), especially the lower one. This perspective also encourages the optimization to locate $x_1, \ldots, x_{m_I}$ according to quadrature schemes inside of D or sample them randomly in the sense of Monte-Carlo-based integral estimates. Finally, the third criterion follows from the properties of our MFS trial functions being particular solutions of (11) in combination with the positively-observable decreasing minimal singular values from (14) which thus serve as trend for the requested vanishing boundary misfit under the boundary-restricted

$\mathcal{H}$-metric. To transfer from these so far tangential-derivatives-free collocation samples to fractional Sobolev norms as required in (*iii*) even more consistently, one could alternatively add higher-order point evaluations to the boundary-related blocks of the discrete operator $\widetilde{T}$ from (12). In total, the statements of Theorem 2 can indeed be considered as the continuous generalization of the modified MFS characteristics.

The sceptical question may arise whether the approximation properties of our translationally-superposed radiating fundamental solutions in focus are sufficient to expect the vanishing-boundary-misfit condition from Theorem 2(*iii*) in the limit $m \longrightarrow \infty$ whenever there is a real ITE to be detected. Since the practically-oriented ansatz (4) is only a discretized version of (7), we will now assume approximate ITP eigenfunctions to be of the more general form

$$v_m = \hat{K}_\kappa g_v^m \qquad \text{and} \qquad w_m = \hat{K}_{\sqrt{n}\kappa} g_w^m \ , \tag{18}$$

where $g_v^m, g_w^m \in L^2(\Gamma)$.

Remark 2. *In order to always refer back from any of the outcomes based on* (18) *in the sequel to the discrete case associated to* (4)*, note that any $h \in \mathcal{A}(\varkappa)$ of the form $h = \hat{K}_\kappa g$ with $g \in L^2(\Gamma)$ can still be approximated by finite linear combinations of translated fundamental solutions even with respect to any $C^\ell(\overline{D})$-norm according to the following procedure: partition Γ into m disjoint connected fractions $\{\gamma_i\}_{1\leq i\leq m}$ with identical arclength and define the approximation kernel $K_\varkappa^m : \Gamma \times D \longrightarrow \mathbb{R}$ by*

$$K_\varkappa^m(x,y) = \sum_{i=1}^m \mathbb{1}_{\gamma_i}(y) K_\varkappa(x, y_{\gamma_i}) \ ,$$

where $\mathbb{1}_{\gamma_i}$ denotes the indicator function on the set γ_i and $y_{\gamma_i} \in \gamma_i$. Analogue to (7) *also the kernel is associated to an operator $\hat{K}_\kappa^m$ generating smooth Helmholtz solutions on $\overline{D}$ by*

$$[\hat{K}_\varkappa^m g](\cdot) := \int_\Gamma K_\varkappa^m(\cdot, y) g(y)\, \mathrm{d}y = \sum_{i=1}^m c_{\gamma_i} K_\varkappa(\cdot, y_{\gamma_i}) \tag{19}$$

with the identification

$$c_{\gamma_i} := \int_{\gamma_i} g(y) \mathrm{d}s(y) \tag{20}$$

in accordance to (4)*. Since $K_\varkappa$ can be reduced to a one dimensional function, whose derivatives up to any order are uniformly continuous for positive arguments exceeding, for instance,* $\mathrm{dist}(\Gamma, \partial D)$*, we may estimate for any integer $\ell \geq 0$*

$$\sup_{x\in\overline{D}} \left| \partial^\ell (\hat{K}_\varkappa^m g - \hat{K}_\varkappa^g) \right| \leq \sup_{x\in\overline{D}} \sum_{i=1}^m \int_{\gamma_i} \left| \partial_x^\ell \big(K_\varkappa(x, y_{\gamma_i}) - K_\varkappa(x,y) \big) \right| |g(y)| \mathrm{d}s(y) \ .$$

Since $\big| |x - y_{\gamma_i}| - |x - y| \big| \leq |y - y_{\gamma_i}|$, there exists a Lipschitz constant $L_\varkappa^\ell$ such that

$$\left| \partial_x^\ell \big(K_\varkappa(x, y_{\gamma_i}) - K_\varkappa(x,y) \big) \right| \leq L_\varkappa^\ell |y - y_{\gamma_i}| \leq \frac{C_\varkappa^\ell}{m}$$

for some $C^\ell_\varkappa > 0$. *Thus the last integral expression can be further estimated, incorporating* $S := \int_\Gamma \mathrm{d}s(y) < \infty$, *by*

$$\sup_{x\in\overline{D}} \left|\partial^\ell (\hat{K}^m_\varkappa g - \hat{K}^g_\varkappa)\right| \leq \sup_{x\in\overline{D}} \sum_{i=1}^m \int_{\gamma_i} \frac{C^\ell_\varkappa |g(y)|}{m} \mathrm{d}s(y) \leq \frac{C^\ell_\varkappa \sqrt{S}\|g\|_{L^2(\Gamma)}}{m} \xrightarrow{m} 0 \ ,$$

where we used the Cauchy-Schwartz inequality in the last step. The discrete approximation assertion for classical norms follows by definition, accumulating the left suprema over ℓ.

Fortunately, we can prove a positive density result for both our discrete and continuous MFS trial functions by tracing back the analysis to the Helmholtz equation. As a first step, let us show that the range of $\hat{K}_\varkappa$ is dense in $\mathcal{A}(\varkappa)$ with respect to $L^2(D)$ for every $\varkappa > 0$ and discuss afterwards how to apply this to the more sophisticated ITP with its coupled boundary data.

Theorem 3. *Let* $\varkappa \in \mathbb{R}_{>0}$ *be any wavenumber and consider the 2D single layer potentials*

$$\hat{K}_\varkappa : L^2(\Gamma) \longrightarrow \mathcal{A}(\varkappa)$$

from (7)*, respectively, whose kernels fulfil the Sommerfeld radiation condition. If* Γ *is of class* C^2, *it holds that the range of* $K_\varkappa$ *is dense in* $\mathcal{A}(\varkappa)$ *with respect to* $L^2(D)$.

Proof. We aim to show that the $L^2(D)$-adjoint of $\hat{K}_\varkappa$ given by

$$\hat{K}^*_\varkappa : L^2(D) \longrightarrow L^2(\Gamma) \ , \qquad [\hat{K}^*_\varkappa h](\cdot) = \int_D \overline{K_\varkappa(\cdot, x)} h(x)\,\mathrm{d}x$$

is injective on $\overline{\mathcal{A}(\varkappa)}$ (the closure taken with respect to $L^2(D)$) which would then give the desired density result according to the fact that the null space of $\hat{K}^*_\varkappa$ equals the $L^2(D)$-orthogonal complement of the range of $\hat{K}_\varkappa$. Hence, we assume that $h \in \overline{\mathcal{A}(\varkappa)}$ is such that $\hat{K}^*_\varkappa h = 0$ which means that the function $\widetilde{h} := \overline{\hat{K}^*_\varkappa h}$, which extends to $\mathbb{R}^2$ naturally as the outcome of a convolution, solves the following equations

$$\begin{aligned} \Delta\widetilde{h} + \varkappa^2\widetilde{h} &= -\overline{h} \quad \text{in } D \\ \Delta\widetilde{h} + \varkappa^2\widetilde{h} &= 0 \quad \text{in } D^{\mathsf{c}} \\ \widetilde{h} &= 0 \quad \text{on } \Gamma \ . \end{aligned}$$

By the theory of volume potentials, we infer that $\widetilde{h} \in H^2_{loc}(\mathbb{R}^2)$ and inherits the Sommerfeld radiation condition from the integral kernel thanks to the additional conjugation within the definition of $\widetilde{h}$. Hence, by uniqueness of the exterior Dirichlet problem for the Helmholtz equation, see for example [10], we may conclude that $\widetilde{h}_{|\Omega^{\mathsf{c}}} = 0$, where Ω is the exhausting set such that $\partial\Omega = \Gamma$. By analyticity, $\widetilde{h}$ also vanishes in D^{c} and can be considered as an element in $H^2_0(D)$. Now by assumption, h is still a distributional solution of the Helmholtz equation with wave number $\varkappa$ in D and may be tested against $\widetilde{h}$ which yields

$$0 = \int_D (\Delta\widetilde{h} + \varkappa^2\widetilde{h}) h \ \mathrm{d}x = -\|h\|_{L^2(D)} \ .$$

As a consequence, $\hat{K}^*_\varkappa$ is injective, or equivalently, $\hat{K}_\varkappa$ has dense range in $\mathcal{A}(\varkappa)$ with respect to $L^2(D)$ and the theorem is proved. □

Remark 3. *Note that in general one cannot waive any additional structure of the fundamental solution kernel $K_\varkappa$ such as the radiating property while keeping the same density results for any admissible Γ. For example, working only with the singular imaginary part of $K_\varkappa$ derived from the first Hankel function, i.e. with Bessel functions of the second kind, in the case of D being a ball surrounded by Γ as a concentrated sphere, its distance to ∂D can be chosen such that our reduced kernel with its source terms on Γ totally vanishes at the midpoint of D. However, since L^2-density results can be extended to local higher order ones including C^0-estimates in the interior as will be demonstrated in the following, we would consequently not be able to approximate Helmholtz functions that vanish at the midpoint in $L^2(D)$ any more.*

Up to now the $\mathcal{A}(\varkappa)$-density properties assured by Theorem 3 for functions generated by (18) are a priori too weak to crush any kind of corresponding boundary approximations down to zero in the limiting process $m \longrightarrow \infty$ with respect to any non-negative Sobolev norm. So we aim to improve the current state endowing the range of $\hat{K}_\varkappa$ more strongly with $H^2(D)$ which still contains the full set of exact ITP solutions according to Lemma 1. In [46] (Theorem 2) Weck showed for positive $\varkappa$ that a similar result indeed holds but he performed the proof for the case of Herglotz wave functions as dense subset in focus, i.e. under the assumption that $K_\varkappa$ in (7) represents planar waves instead of translated fundamental solutions. His main idea was to construct via a clever fixed point argument for any $h \in \mathcal{A}(\varkappa)$ a $H^2(D)$-convergent sequence of smooth Helmholtz solutions h_m living on slightly larger domains D_m and which can be reapproximated on $D \subset\subset D_m$ by Herglotz wave functions via higher order interior estimates bounded in terms of the augmented $L^2(D_m)$-norm by ellipticity. Fortunately, the only Herglotz-specific fact that Weck utilized while proving the latter was an initial L^2 density result analogue to ours (with D replaced by D_m in our Theorem 3 for m large in order not to intersect with Γ) and regularity assumptions on D which therefore enable us to directly adopt these findings to our MFS framework, too. We summarize them in the following corollary and relist all necessary requirements:

Corollary 4. *Let Γ be of class C^2, ∂D be of class C^4 and assume that n is constant within D. Then, for any positive ITE k the assumptions of Theorem 2 can be fulfilled by approximate functions (v_m, w_m) of the form (18) whose Helmholtz kernels are radiating. In particular, the extended MFS embedded in $\mathcal{H}$ is capable for detecting all real-valued ITEs.*

Proof. Let k be any positive ITE and (v, w) any corresponding eigenfunction pair fulfilling (2). According to Lemma 1, v and w are each smooth solutions of the Helmholtz equation and due to our recent density improvement adopted from [46] there exist sequences $\{v_m\}_{m\in\mathbb{N}}$, $\{w_m\}_{m\in\mathbb{N}}$ of the form (18) approximating v and w with respect to $H^2(D)$, respectively. In particular, if we set $k_m := k$ for all $m \in \mathbb{N}$ we obtain for a domain specific constant $c > 0$

$$
\begin{aligned}
&\|v_m - w_m\|_{H^{\frac{3}{2}}(\partial D)} + \|\partial_\nu(v_m - w_m)\|_{H^{\frac{1}{2}}(\partial D)} \\
\leq &\|v_m - v\|_{H^{\frac{3}{2}}(\partial D)} + \|w - w_m\|_{H^{\frac{3}{2}}(\partial D)} + \|\partial_\nu(v_m - v)\|_{H^{\frac{1}{2}}(\partial D)} + \|\partial_\nu(w - w_m)\|_{H^{\frac{1}{2}}(\partial D)} \\
\leq &c\left(\|v_m - v\|_{H^2(D)} + \|w_m - w\|_{H^2(D)}\right) \longrightarrow 0
\end{aligned}
$$

and

$$\begin{aligned} 0 < C^{-1} &< \liminf_{m\to\infty}(\|v_m\|_{L^2(D)} + \|w_m\|_{L^2(D)}) = \|v\|_{L^2(D)} + \|w\|_{L^2(D)} \\ &= \limsup_{m\to\infty}(\|v_m\|_{L^2(D)} + \|w_m\|_{L^2(D)}) < C \end{aligned}$$

for some proper $C > 1$. □

A last subtlety should be mentioned about the previous corollary when dealing with approximations under finite precision arithmetics. If k is any ITE with eigenfunction pair (v, w), then we know that there is a sequence of coefficient functions $\{(g_v^m, g_w^m)\}_{m\in\mathbb{N}} \subset L^2(\Gamma)$ and discretized operators $\{(\widehat{K}_\kappa^m, \widehat{K}_{\sqrt{n}\kappa}^m)\}_{m\in\mathbb{N}}$ as in (19) such that

$$\begin{aligned} \widehat{K}_\kappa^m g_v^m &\longrightarrow v \ , \\ \widehat{K}_{\sqrt{n}\kappa}^m g_w^m &\longrightarrow w \ , \end{aligned}$$

with respect to any of the infinite dimensional norms we discussed above. The attendant errors for fixed m are unavoidable in the left hand sides but they still approach zero in the limiting process. Note by compactness of the operators involved we cannot transfer back to any relation among the coefficient functions $\{(g_v^m, g_w^m)\}_{m\in\mathbb{N}}$. The worst-case scenario occurs if computational rounding errors come into play and (v, w) is not in the operator range itself but only in the closure which implies $\|g_v^m\|_{L^2(\Gamma)} \longrightarrow \infty$ or $\|g_w^m\|_{L^2(\Gamma)} \longrightarrow \infty$. Assume without loss of generality the first case and that $\widetilde{K}_\kappa^m$ is a slight perturbation of $\widehat{K}_\kappa^m$. Denoting by ϵ_m the operator misfit in terms of any convenient metric, the potential total error between the eigenfunction reapproximations, here $\widehat{K}_\kappa^m g_v^m$ and $\widetilde{K}_\kappa^m g_v^m$, would be of order ϵ_m times the norm of $\|g_v^m\|_{L^2(\Gamma)}$ where the latter blows up by assumption.

However, hope is given in practice if we have a closer look on the relation between the exploding coefficient functions g_v^m and their discrete equivalents denoted by c_v^m in the style of (20). Then the length of the corresponding average fractions γ_i scales like m^{-1}, so we may infer with Jensen's inequality

$$\begin{aligned} |c_v^m|^2 &= \sum_{i=1}^m \left(\int_{\gamma_i} g_v^m(y)\,\mathrm{d}s(y)\right)^2 = \sum_{i=1}^m \mathcal{H}^1(\gamma_i)^2 \left(\frac{1}{\mathcal{H}^1(\gamma_i)}\int_{\gamma_i} g_v^m(y)\,\mathrm{d}s(y)\right)^2 \\ &\leq \sum_{i=1}^m \frac{\mathcal{H}^1(\Gamma)}{m}\int_{\gamma_i} g_v^m(y)^2\,\mathrm{d}s(y) = \frac{\mathcal{H}^1(\Gamma)}{m}\sum_{i=1}^m \int_{\gamma_i} g_v^m(y)^2\,\mathrm{d}s(y) = \frac{\mathcal{H}^1(\Gamma)}{m}\|g_v^m\|_{L^2(\Gamma)}^2 \ . \end{aligned}$$

Hence, if the coefficient functions do not grow stronger than the square root of m, the discrete MFS should effectively be invisible with respect to L^2-norm blow-ups and the transferred vector norm keeps uniformly bounded in m. Consequently, in agreement with Barnett and Betcke's observation from [3], for practical applications of the modified MFS we expect absolute errors in the boundary approximations to be finally limited by the order of ϵ_m, i.e. machine precision, times the uniform coefficient vector bound, if the latter exists.

It now appears natural to seek for an estimate which bounds the absolute error between approximate and its corresponding exact eigenvalue in terms of the boundary misfit of the approximate eigenfunctions. This will be done again in the continuous framework and holds as long as some vanishing integral constraint is disobeyed. Such a

relation also justifies heuristically why in our numerical experiments from the previous section it was mostly observed that the smaller the computed minimal singular value from (13) is (or equivalently the discrete boundary misfit according to (14)), the better the accuracy of the approximate eigenvalue becomes. Furthermore, note that eigenvalue deviations will already be controlled in the corresponding weaker norms $L^2(\partial D)$ which is more in the spirit of our discretized MFS output data unlike the more sophisticated $\mathcal{H}$-measurements in Theorem 2 necessary to prove that accumulation points of $\{k_m\}_{m\in\mathbb{N}}$ are indeed unpolluted ITEs.

Lemma 5. *Let (v,w) be an ITP eigenfunction pair with ITE k and assume that $(\widetilde{v},\widetilde{w})\in\mathcal{H}(\widetilde{k})$ under the same index of refraction n. If*

$$\left|\int_D (v\widetilde{v}-nw\widetilde{w})\,\mathrm{d}x\right| \geq \widetilde{\varepsilon}\neq 0\ ,$$

then there exists a constant $\widetilde{C}>0$ which depends only on the boundary data of v,w and on $\widetilde{\varepsilon}$ such that for all $(\widetilde{v},\widetilde{w})$ with the above $\widetilde{\varepsilon}$-property it holds that

$$|k^2-\widetilde{k}^2|\leq \widetilde{C}\sqrt{\|\widetilde{v}-\widetilde{w}\|^2_{L^2(\partial D)}+\|\partial_\nu(\widetilde{v}-\widetilde{w})\|^2_{L^2(\partial D)}}\ . \tag{21}$$

Proof. Integration by parts in combination with the Helmholtz equation yields

$$\begin{aligned}
&k^2\int_D(\widetilde{v}v-n\widetilde{w}w)\,\mathrm{d}x\\
&=\int_D(-\widetilde{v}\Delta v+\widetilde{w}\Delta w)\,\mathrm{d}x\\
&=\int_D\nabla\widetilde{v}\cdot\nabla v\,\mathrm{d}x-\int_D\nabla\widetilde{w}\cdot\nabla w\,\mathrm{d}x-\int_{\partial D}(\widetilde{v}-\widetilde{w})\underbrace{\partial_\nu w}_{=\partial_\nu v}\,\mathrm{d}s\\
&=\int_D(-v\Delta\widetilde{v}+w\Delta\widetilde{w})\,\mathrm{d}x+\int_{\partial D}\partial_\nu(\widetilde{v}-\widetilde{w})w\,\mathrm{d}s-\int_{\partial D}(\widetilde{v}-\widetilde{w})\partial_\nu w\,\mathrm{d}s\\
&=\widetilde{k}^2\int_D(\widetilde{v}v-n\widetilde{w}w)\,\mathrm{d}x+\int_{\partial D}\partial_\nu(\widetilde{v}-\widetilde{w})w\,\mathrm{d}s-\int_{\partial D}(\widetilde{v}-\widetilde{w})\partial_\nu w\,\mathrm{d}s\ ,
\end{aligned}$$

or equivalently in rearranged form

$$(k^2-\widetilde{k}^2)\int_D(\widetilde{v}v-n\widetilde{w}w)\,\mathrm{d}x=\int_{\partial D}\partial_\nu(\widetilde{v}-\widetilde{w})w\,\mathrm{d}s-\int_{\partial D}(\widetilde{v}-\widetilde{w})\partial_\nu w\,\mathrm{d}s\ .$$

Taking absolute values gives

$$\left|k^2-\widetilde{k}^2\right|\leq\frac{1}{\widetilde{\varepsilon}}\left(\int_{\partial D}|\partial_\nu(\widetilde{v}-\widetilde{w})w|\,\mathrm{d}s+\int_{\partial D}|(\widetilde{v}-\widetilde{w})\partial_\nu w|\,\mathrm{d}s\right)$$

and applying the Cauchy Schwartz inequality twice results in

$$\begin{aligned}
\left|k^2-\widetilde{k}^2\right|&\leq\frac{1}{\widetilde{\varepsilon}}\left(\|\partial_\nu(\widetilde{v}-\widetilde{w})\|_{L^2(\partial D)}\|w\|_{L^2(\partial D)}+\|\widetilde{v}-\widetilde{w}\|_{L^2(\partial D)}\|\partial_\nu w\|_{L^2(\partial D)}\right)\\
&\leq\frac{\sqrt{\|w\|^2_{L^2(\partial D)}+\|\partial_\nu w\|^2_{L^2(\partial D)}}}{\widetilde{\varepsilon}}\sqrt{\|\widetilde{v}-\widetilde{w}\|^2_{L^2(\partial D)}+\|\partial_\nu(\widetilde{v}-\widetilde{w})\|_{L^2(\partial D)}\|^2}\ .
\end{aligned}$$

Obviously, we may choose $\widetilde{C}:=\frac{\sqrt{\|w\|^2_{L^2(\partial D)}+\|\partial_\nu w\|^2_{L^2(\partial D)}}}{\widetilde{\varepsilon}}<\infty$ and the lemma is proven. □

As the applicability of (21) depends on the compliance of the integral constraint for each approximate eigenfunction pair, the following corollary shifts this responsibility for ITE approximations based on the extended MFS procedure embedded in $\mathcal{H}$, cf. Theorem 2, only to the limitting eigenfunction. Note that the delicate minus sign within the definition of $\widetilde{\varepsilon}$ is still due to the non-elliptic nature of the interior transmission problem.

Corollary 6. *Let the conditions of Theorem 2 hold for (v, w) and let (v', w') be any (other) solution of the ITP with identical ITE k. Assume that the following non-vanishing integral relation is satisfied*

$$\int_D (vv' - nww') \,\mathrm{d}x \neq 0 \ . \tag{22}$$

Then, for sufficiently large $m \in \mathbb{N}$, the approximate ITEs k_m associated to the constructed, weakly convergent subsequence of $\{(v_m, w_m)\} \subset \mathcal{H}$ from Theorem 2 are controlled by

$$\begin{aligned} |k^2 - k_m^2| &\leq C \sqrt{\|v_m - w_m\|^2_{L^2(\partial D)} + \|\partial_\nu (v_m - w_m)\|^2_{L^2(\partial D)}} \\ &\leq C \sqrt{\|v_m - w_m\|^2_{H^{\frac{3}{2}}(\partial D)} + \|\partial_\nu (v_m - w_m)\|^2_{H^{\frac{1}{2}}(\partial D)}} \ , \end{aligned} \tag{23}$$

where $C > 0$ only depends on v', w' and the magnitude of (22).

Proof. By weak convergence we know that

$$\int_D (v_m v' - n w_m w') \,\mathrm{d}x \longrightarrow \int_D (vv' - nww') \,\mathrm{d}x \neq 0 \ .$$

Thus for large m and some $\widetilde{\varepsilon} > 0$ it must also hold that

$$\left| \int_D (v_m v' - n w_m w') \,\mathrm{d}x \right| \geq \widetilde{\varepsilon} \ , \tag{24}$$

so the assertion follows with Lemma 5. □

Remark 4. *We verified numerically for our primary benchmark case with parameters $n = 4$ and the smallest real-valued ITE of the unit disc $k \approx 2.902608055212766$ that the integral from* (22)*, choosing $v = v', w = w'$ based on* (10) *with index $p = 1$ and $c_1^w = 1$, is indeed bounded away from zero and we may choose $\widetilde{\varepsilon} > 0.453$. Since the associated Bessel functions of the first kind are smooth, all assumptions are fulfilled such that* (24) *can be positively applied in this ITP case. Certainly, one does normally not know any properties of the underlying ITP eigenvector pair a priori, so the derived ITE estimate might not be feasible in general.*

Remark 5. *In [5], facing the Laplacian Dirichlet eigenvalue problem, Betcke & Trefethen relate the problem of finding MPS-based approximations with least boundary norm to the concept of subspace angles between functions satisfying the interior κ-dependent eigenvalue relation and those having zero boundary data, respectively. Obviously, if the two subspaces have a non-trivial intersection for some k, it is spanned by the corresponding Dirichlet eigenfunctions. It is possible to adopt this perspective*

also for the ITP case. A convenient definition of the subspace angle φ between the function spaces $\mathcal{A}$ and $\mathcal{D}$ would be

$$\cos(\varphi) := \sup_{a\in\mathcal{A},b\in\mathcal{D}} \frac{(a,b)_{\mathcal{H}}}{\|a\|_{\mathcal{H}}\|b\|_{\mathcal{H}}} ,$$

where $\|\cdot\|_{\mathcal{H}}$ is the induced norm from the inner product (16)*. We may define $\mathcal{A} = \mathcal{H}(\kappa)$ as the set of 2-tuples solving* (2) *and $\mathcal{D}$ as those functions pairs having identical Neumann and Dirichlet boundary data. In coincidence with the Dirichlet case, simple algebraic manipulations finally show that the sine of $\varphi = \varphi(\kappa)$ then equals the minimal boundary misfit of $\|\cdot\|_{\mathcal{H}}$-normed functions from $\mathcal{H}(\kappa)$ when measured in terms of the boundary part of our underlying inner product. As a consequence, the right hand side of* (23) *is then equivalently bounded in terms of the subspace angle between $\mathcal{H}(k_m)$ and $\mathcal{D}$.*

5. Conclusions

We applied the method of fundamental solutions in two different versions for the computation of interior transmission eigenvalues from homogeneous scatterers in 2D. We showed that it is theoretically capable for detecting all real-valued ITEs if the scattering boundary is sufficiently smooth and proved auxiliary error estimates which are controlled by some generalized MFS output. Our second implementation, which is based on the interior point extension with an additional QR decomposition from [5] to overcome severe ill-conditioning effects, turns out to be the most convenient and robust way for ITE approximations with fundamental solutions as starting point. As such, our final algorithm is still easy-to-implement and manages to achieve high accuracy mostly up to machine precision for scatterers which are relatively similar to the disc. However, the approximation quality tends to degenerate within our numerical experiments in correlation with the domain's complexity when restricting to circles as the only surrounding source point contours. The more general case is not yet covered by our presented analysis and will be the focus of future research as well as a concrete MFS-specific convergence analysis whose rates we also believe to depend on the source locations and on continuation properties of the corresponding ITP eigenfunctions.

References

[1] S. Agmon. *Lectures on Elliptic Boundary Value Problems.* American Mathematical Soc., Heidelberg, 2010.

[2] L. Audibert. *Qualitative methods for heterogeneous media.* PhD thesis, Ecole Doctorale Polytechnique, 2015.

[3] A. H. Barnett and T. Betcke. Stability and convergence of the method of fundamental solutions for Helmholtz problems on analytic domains. *Journal of Computational Physics*, 227(14):7003–7026, 2008.

[4] T. Betcke. The generalized singular value decomposition and the method of particular solutions. *SIAM Journal on Scientific Computing*, 30(3):1278–1295, 2008.

[5] T. Betcke and L. N. Trefethen. Reviving the method of particular solutions. *SIAM Review*, 47(3):469–491, 2005.

[6] W.-J. Beyn. An integral method for solving nonlinear eigenvalue problems. *Linear Algebra and Its Applications*, 436(10):3839–3863, 2012.

[7] E. Blåsten, X. Li, H. Liu, and Y. Wang. On vanishing and localizing of transmission eigenfunctions near singular points: a numerical study. *Inverse Problems*, 33(10):105001, 2017.

[8] E. Blåsten, L. Päivärinta, and J. Sylvester. Corners always scatter. *Communications in Mathematical Physics*, 331:725–753, 2014.

[9] F. Cakoni, M. Cayoren, and D. Colton. Transmission eigenvalues and the nondestructive testing of dielectrics. *Inverse Problems*, 24(15):065016, 2008.

[10] F. Cakoni and D. Colton. *Qualitative Methods in Inverse Scattering Theory - An Introduction*. Springer, Berlin, 2005.

[11] F. Cakoni, D. Colton, and H. Haddar. On the determination of Dirichlet or transmission eigenvalues from far field data. *Comptes Rendus Mathematique*, 348(7–8):379–383, 2010.

[12] F. Cakoni, D. Colton, and H. Haddar. *Inverse Scattering Theory and Transmission Eigenvalues*. SIAM, Philadelphia, 2016.

[13] F. Cakoni, M. Fares, and H. Haddar. Analysis of two linear sampling methods applied to electromagnetic imaging of buried objects. *Inverse Problems*, 22(3):845–867, 2006.

[14] F. Cakoni and H. Haddar. Transmission eigenvalues in inverse scattering theory, 2012.

[15] F. Cakoni and R. Kress. A boundary integral equation method for the transmission eigenvalue problem. *Applicable Analysis*, 96(1):23–38, 2017.

[16] D. Colton and Y.-J. Leung. Complex transmission eigenvalues for spherically stratified media. *Inverse Problems*, 28(7):075005, 2012.

[17] D. Colton and Y.-J. Leung. The existence of complex transmission eigenvalues for spherically stratified media. *Applicable Analysis*, 96(1):39–47, 2017.

[18] D. Colton, Y.-J. Leung, and S. Meng. Distribution of complex transmission eigenvalues for spherically stratified media. *Inverse Problems*, 31(3):035006, 2015.

[19] D. Colton and P. Monk. The inverse scattering problem for time-harmonic acoustic waves. *SIAM Review*, 26(3):323–350, 1984.

[20] D. Colton, P. Monk, and J. Sun. Analytical and computational methods for transmission eigenvalues. *Inverse Problems*, 26(4):045011, 2010.

[21] A. Cossonnière. *Valeurs propres de transmission et leur utilisation dans l'identification d'inclusions à partir de mesures électromagnétiques*. PhD thesis, Toulouse, 2011.

[22] A. Cossonnière and H. Haddar. Surface integral formulation of the interior transmission problem. *Journal of Integral Equations and Applications*, 25(3):341–376, 2013.

[23] L. Fox, P. Henrici, and C. Moler. Approximations and bounds for eigenvalues of elliptic operators. *SIAM Journal on Numerical Analysis*, 4(1):89–102, 1967.

[24] H. Geng, X. Ji, J. Sun, and L. Xu. C^0IP methods for the transmission eigenvalue problem. *Journal of Scientific Computing*, 68(1):326–338, 2016.

[25] D. Gilbarg and N. S. Trudinger. *Elliptic Partial Differential Equations of Second Order*. Springer, Berlin, 2015.

[26] D. Gintides and N. Pallikarakis. A computational method for the inverse transmission eigenvalue problem. *Inverse Problems*, 29(10):104010, 2013.

[27] J. Han and Y. Yang. An adaptive finite element method for the transmission eigenvalue problem. *Journal of Scientific Computing*, 69(3):1279–1300, 2016.

[28] J. Han and Y. Yang. An H^m-conforming spectral element method on multi-dimensional domain and its application to transmission eigenvalues. *Science China Mathematics*, 60(8):1529–1542, 2017.

[29] J. Han, Y. Yang, and H. Bi. A new multigrid finite element method for the transmission eigenvalue problems. *Applied Mathematics and Computation*, 292:96–106, 2017.

[30] X. Ji and J. Sun. A multi-level method for transmission eigenvalues of anisotropic media. *Journal of Computational Physics*, 255:422–435, 2013.

[31] X. Ji, J. Sun, and H. Xie. A multigrid method for Helmholtz transmission eigenvalue problems. *Journal of Scientific Computing*, 60(2):276–294, 2014.

[32] A. Kirsch. The denseness of the far field patterns for the transmission problem. *IMA Journal of Applied Mathematics*, 37(3):213–225, 1986.

[33] A. Kirsch and N. Grinberg. *The Factorization Method for Inverse Problems*. Oxford University Press, Oxford, 2008.

[34] A. Kirsch and A. Lechleiter. The inside–outside duality for scattering problems by inhomogeneous media. *Inverse Problems*, 29(10):104011, 2013.

[35] A. Kleefeld. A numerical method to compute interior transmission eigenvalues. *Inverse Problems*, 29(10):104012, 2013.

[36] A. Kleefeld. *Numerical methods for acoustic and electromagnetic scattering: Transmission boundary-value problems, interior transmission eigenvalues, and the factorization method*. Habilitation thesis, Brandenburg University of Technology Cottbus-Senftenberg, 2015.

[37] A. Lechleiter and S. Peters. Analytical characterization and numerical approximation of interior eigenvalues for impenetrable scatterers from far fields. *Inverse Problems*, 30(4):045006, 2014.

[38] H. Li and Y. Yang. An adaptive C^0IPG method for the Helmholtz transmission eigenvalue problem. *arXiv:1708.06104*, 2017.

[39] T. Li, T.-M. Huang, W.-W. Lin, and J.-N. Wang. An efficient numerical algorithm for computing densely distributed positive interior transmission eigenvalues. *Inverse Problems*, 33(3):035009, 2017.

[40] T. Li, W.-Q. Huang, W.-W. Lin, and J. Liu. On spectral analysis and a novel algorithm for transmission eigenvalue problems. *Journal of Scientific Computing*, 64(1):83–108, 2015.

[41] J. L. Lions and E. Magenes. *Non-Homogeneous Boundary Value Problems and Applications*. Springer, Berlin, 2012.

[42] R. Mennicken and M. Möller. *Non-self-adjoint boundary eigenvalue problems*, volume 192. Gulf Professional Publishing, 2003.

[43] J. Sun. Iterative methods for transmission eigenvalues. *SIAM Journal on Numerical Analysis*, 49(5):1860–1874, 2011.

[44] J. Sun and A. Zhou. *Finite Element Methods for Eigenvalue Problems*. CRC Press, Boca Raton, 2017.

[45] G. Vodev. Transmission eigenvalue-free regions. *Communications in Mathematical Physics*, 336(3):1141–1166, 2015.

[46] N. Weck. Approximation by Herglotz wave functions. *Mathematical Methods in the Applied Sciences*, 27(2):155–162, 2004.

[47] Y. Xi and X. Ji. Recursive integral method for the nonlinear non-selfadjoint transmission eigenvalue problem. *Journal of Computational Mathematics*, 35(6):828–838, 2017.

[48] Y. Xi, X. Ji, and S. Zhang. A multi-level mixed element scheme of the two dimensional helmholtz transmission eigenvalue problem. *arXiv:1707.00567*, 2017.

[49] H. Xie and X. Wu. A multilevel correction method for interior transmission eigenvalue problem. *Journal of Scientific Computing*, 72(2):586–604, 2017.

[50] X.-C. Xu, C.-F. Yang, S. A. Buterin, and V. A. Yurko. Estimates of complex eigenvalues and an inverse spectral problem for the transmission eigenvalue problem. *arXiv:1703.01709*, 2017.

[51] Y. Yang, H. Bi, H. Li, and J. Han. Mixed methods for the Helmholtz transmission eigenvalues. *SIAM Journal on Scientific Computing*, 38(3):A1383–A1403, 2016.

[52] Y. Yang, H. Bi, H. Li, and J. Han. A C^0IPG method and its error estimates for the Helmholtz transmission eigenvalue problem. *Journal of Computational and Applied Mathematics*, 326:71–86, 2017.

[53] Y. Yang, J. Han, and H. Bi. Error estimates and a two grid scheme for approximating transmission eigenvalues. *arXiv:1506.06486*, 2016.

[54] Y. Yang, J. Han, and H. Bi. Non-conforming finite element methods for transmission eigenvalue problem. *Computer Methods in Applied Mechanics and Engineering*, 307:144–163, 2016.

[55] F. Zeng, J. Sun, and L. Xu. A spectral projection method for transmission eigenvalues. *Science China Mathematics*, 59(8):1613–1622, 2016.